Progress In Electromagnetics Research B, Vol. 23, 273–291, 2010

OPTICAL PERFORMANCE ANALYSIS USING A POINT SPREAD FUNCTION AND MODULATION TRANSFER FUNCTION FOR W-BAND PMMW IMAGING SYSTEM BASED ON QUASI OPTICS FOCUSED ARRAY OF DIELECTRIC ROD WAVEGUIDE ANTENNA

M. K. Singh and W.-G. Kim

Microwave Sensor System Laboratory
School of Information and Mechatronics
Gwangju Institute of Science and Technology (GIST)
261 Chemdan-gwagiro, Buk-Gu, Gwangju 500 712, Republic of Korea

U. S. Tiwary

Indian Institute of Information Technology
Allahabad, India

S.-J. Lee and D.-R. Cho

Agency for Defense Development
Republic of Korea

Y.-H. Kim

Microwave Sensor System Laboratory
School of Information and Mechatronics
Gwangju Institute of Science and Technology (GIST)
261 Chemdan-gwagiro, Buk-Gu, Gwangju 500 712, Republic of Korea

Abstract—The appropriateness of dielectric loaded antenna for the passive millimeter wave imaging application has recently been demonstrated. In this paper, we analyze the optical performance of the passive millimeter wave (PMMW) imaging system based on a 1D focal plane array (FPA) of dielectric rod waveguide (DRW) antennas. A first step in the design process is to analyze the image quality potential of 1D FPA-based imaging system in terms of the point spread function (PSF) and the modulation transfer function (MTF). We consider the effect

Received 20 April 2010, Accepted 2 July 2010, Scheduled 25 July 2010
Corresponding author: Y.-H. Kim (yhkim@gist.ac.kr).

of lens, DRW antenna, electromagnetic crosstalk between adjacent DRW antenna elements in the array, and sampling. From simulation and measurement, we found that the image quality in the passive millimeter wave imaging system with a DRW antenna array is less sensitive to electromagnetic crosstalk between antenna elements in the array. The measurements and simulations show that the system is diffraction limited and also closely agrees with the *Rayleigh criterion* of resolution for diffraction limited optical systems.

1. INTRODUCTION

Millimeter wave sensors have been used for decades for various applications such as military radar and radiometry, metrological applications, radio astronomy, earth resource monitoring, medical applications, and more recently for concealed weapon detection [1–3]. Passive millimeter wave imaging is a method of forming an image through the passive detection of naturally occurring millimeter wave radiation from an object. This imaging is typically performed using a single or a linear array of the focused detector[†] to raster scan the scene [4, 5]. The PMMW camera was also developed using the same configuration similar to what is commonly used in visible and IR camera [6, 7], i.e., the 2D array of the focused detector [6–12].

In order to get a high resolution millimeter wave image, various types of detectors have been tried for the feed element in the focal plane array (FPA) based quasi optical imaging systems at W-band [8–14]. The spatial resolution of a focal plane array system very much depends on the spacing of its feed elements in the detector array. Therefore, a feed with very low cross section is required. On the other hand, the feed must provide the spillover losses as low as possible. However, this requires a highly directive antenna which would usually have a larger cross section. So, it is quite challenging to design the suitable array elements that can meet these competing requirements. The spillover argument is made from the far-field assumption as is done in the paper based on [20]. The inherent limitations, such as small f-number, of millimeter wave optics also put constraint on achievable spatial resolution.

Antennas fabricated on planar substrates have been tried by many researchers [8–12]. Despite the compact size of a planar antenna array on substrate, one important limitation of this type of antenna array is the loss caused by surface waves propagating along the substrate. The detector on substrate often excites trapped surface

[†] Detector refers as a front end of a receiver not microwave detector.

waves that reduce the radiation efficiency and causes crosstalk between neighboring detectors in the array. More than 50% of incident power can be lost into surface wave [8]. The lost power is captured by the neighboring detector and causes strong crosstalk. Therefore, such a detector introduces a large amount of blurring in the image due to high crosstalk and the image quality is very poor. The excitation of surface waves can be reduced by making the substrate very thin, but the fabrication becomes difficult and mechanically unstable. An alternative solution suggested in [8] is the use of an additional substrate lens on detector array. It is reported in [8] that the use of additional substrate lens on top of the substrate reduces the crosstalk between nearest neighbor detector about −19 dB, but it is still high for the imaging application. This additional lens makes system heavy and also introduces material and reflection loss when the number of detector increases.

So far the most practical structure is a dielectric rod antenna due to their low cross polarization, relatively high gain and potential for a very dense packaging. We developed modified tapered dielectric rod waveguide (DRW) antenna [15] as shown in Figure 1(a), for the efficient use as a feed element in antenna array. Using this feed antenna, we developed an efficient and high performance 30 element feed linear array as shown in Figure 1(b) for quasi optical passive imaging system based on focal plane array (FPA).

One of the objectives of this paper is to evaluate the imaging performance of the proposed quasi optics for W-band PMMW imaging. We evaluated the performance of the developed quasi optics (lens [16] + DRW antenna array) using point spread function (PSF) and modulation transfer function (MTF). We found by simulation and experiment that crosstalk is very less (approximately −39 dB) in the

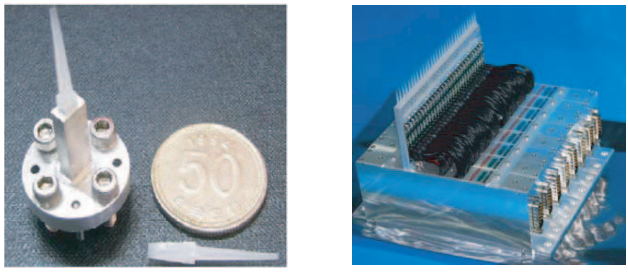

(a) (b)

Figure 1. (a) Designed DRW antenna and (b) 30 elements feed linear DRW antenna array and W-band receivers. (By permission Millisys, Inc., South Korea).

proposed linear feed array based on DRW antenna. An improvement of 20 dB is achieved over the planar antenna array on substrate [8].

Another objective of this paper is to analyze the combined effect of each subsystem in terms of their PSF and MTF for W-band PMMW imaging system, as shown in Figure 2. In this paper, we use the line scan W-band PMMW imaging system and assume the linear shift invariant system model for the mathematical formulation. The intent of this paper is to rigorously develop an approach to PSF and MTF analysis for shift invariant W-band PMMW imaging system as shown in Figure 2 and to analyze the loss of resolution due to the combined effect of lens, focal plane array, and sampling. The measurement setup for PSF is presented and the diffraction limited nature of the proposed system is analyzed.

The rest of the paper is organized as follows. Section 2 describes the PSF and MTF of W-band PMMW imaging system. Section 3 presents the PSF and MTF of the designed dielectric lens [16], developed linear array of DRW antenna. Section 4 presents the PSF measurement setup and the optical performance analysis followed by conclusion in Section 5.

2. PSF AND MTF OF W-BAND PMMW IMAGING SYSTEM

It is widely accepted that the point spread function (PSF) and their Fourier transforms, the modulation transfer functions (MTF), is the fundamental analysis tool for initial imaging system specification and design, perfomence analysis, and subsequent detail analysis of image it produces. A general schematic of sampled W-band PMMW imaging system is shown in Figure 2. The imaging subsystem PSF's (lens + DRW antenna array), the sampling subsystem PSF's, and the reconstruction subsystem PSF's are the components that apply to all system. In this paper, we consider analysis up to sampling subsystem. The imaging system is assumed to be linear and shift invariant; thus the convolution of subsystems PSF's provide the overall PSF of the sampled imaging system used for performance analysis. The output final output of the system in Figure 2 is given by:

$$g_r(x,y) = [\{(I(x,y) \otimes h(x,y)) \otimes h_{sh}(x,y)\} K(x,y)] \otimes h_r(x,y), \quad (1)$$

where $\otimes$ denote the convolution operator.

The receiver channel response, $K(x,y)$, is linear and each channel has its own gain and offset. In the developed PMMW imaging system, every channel of the receiver is calibrated and normalized for flat field response before image reconstruction, thus, $K(x,y)$ is eliminated

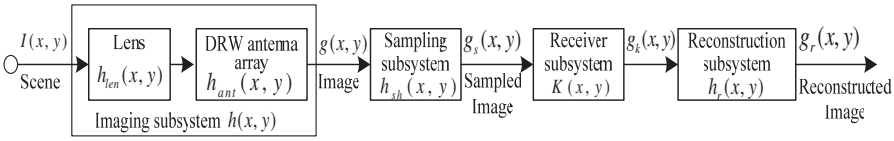

Figure 2. W-band PMMW imaging system.

from Eq. (1). After eliminating $K(x, y)$ and using associative and commutative property of convolution in Eq. (1), we get following simplified form of Eq. (1):

$$g_r(x, y) = \{h(x, y) \otimes h_{sh}(x, y) \otimes h_r(x, y)\} \otimes I(x, y). \tag{2}$$

The imaging subsystem PSF, $h(x, y)$, is given by convolution of lens PSF, $h_{len}(x, y)$, and antenna array PSF, $h_{Ant}(x, y)$:

$$h(x, y) = h_{len}(x, y) \otimes h_{Ant}(x, y). \tag{3}$$

The lens PSF is given by convolution of its diffraction PSF, $h_{diff}(x, y)$, and geometrical aberration PSF, $h_{geom}(x, y)$, i.e., $h_{len}(x, y) = h_{diff}(x, y) \otimes h_{geom}(x, y)$.

Here, it is important to note that the present focal-plane configuration is an array of independent dielectric rod waveguide (DRW) antenna. The output of channel does not depend on the phase coherence between signals on adjacent channels, because, each antenna feeds has its own individual receiver. The PSF of individual antenna in focal plane array, $h_{Ant}(x, y)$, is the convolution of PSF corresponding to the spatial responsivity, i.e., DRW antenna radiation pattern $h_{\mathrm{DRW}}(x, y)$, and PSF $h_{crt}(x, y)$ corresponding to the crosstalk. The individual antenna PSF in focal plane array is $h_{Ant}(x, y) = h_{\mathrm{DRW}}(x, y) \otimes h_{crt}(x, y)$. The imaging subsystem PSF, $h(x, y)$, is given as:

$$h(x, y) = h_{diff}(x, y) \otimes h_{geom}(x, y) \otimes h_{\mathrm{DRW}}(x, y) \otimes h_{crt}(x, y). \tag{4}$$

Convolution in spatial domain corresponds to multiplication in the frequency domain. Thus, equivalent of Eq. (2) and Eq. (4) in frequency domain is as follows:

$$G_r(x, y) = \{H(\xi, \eta) H_{sh}(\xi, \eta) H_r(\xi, \eta)\} I(\xi, \eta), \tag{5}$$

$$H(\xi, \eta) = H_{diff}(\xi, \eta) H_{geom}(\xi, \eta) H_{\mathrm{DRW}}(\xi, \eta) H_{crt}(\xi, \eta). \tag{6}$$

It is obvious from the definition of MTF that the capital H's are MTF corresponding to the PSF denoted by small h's. Eq. (4), Eq. (5) and Eq. (6) are the basis for all the analysis in this paper. Moreover, the results of this paper are applicable to the MTF analysis of any sampled imaging system whose performance is characterized by these equations.

3. PSF AND MTF MODELING FOR W-BAND PMMW IMAGING SYSTEM

3.1. Optical PSF and MTF

There are two physical processes related to the lens that account for the optical blurring and degradation in an imaging system: Diffraction and aberrations. The degradations associated with diffraction and aberration is called diffraction blur and geometric blur, respectively.

3.1.1. Lens Diffraction PSF and MTF

The diffraction accounts for the spreading of the radiation as it passes through an aperture. Thus, a point object is never imaged on a point in the image plane, as shown in Figure 3. The diffraction PSF for an incoherent imaging system with circular-aperture lens of diameter D is given as follows [17–19]:

$$h_{diff}(x,y) = \left| \frac{2J_1(\pi\rho)}{\pi\rho} \right|^2, \tag{7}$$

where J_1 is the first order Bessel function of first kind, $\rho = rD/\lambda f$ is the normalized radial distance from the center of the pattern. λ is the wavelength, $r = \sqrt{x^2 + y^2}$, and f is the focal length of the lens.

The MTF corresponding to the diffraction PSF is obtained by taking the Fourier transform of the function in Eq. (7). The diffraction MTF is given as follows [17]:

$$H_{diff}(\xi,\eta) = \frac{2}{\pi}\left[\cos^{-1}\left(\frac{w\lambda}{D}\right) - \left(\frac{w\lambda}{D}\right)\sqrt{1-\left(\frac{w\lambda}{D}\right)^2}\right], \tag{8}$$

where, $w = \sqrt{\xi^2 + \eta^2}$, and its unit is cycle per mm or cycle per radian.

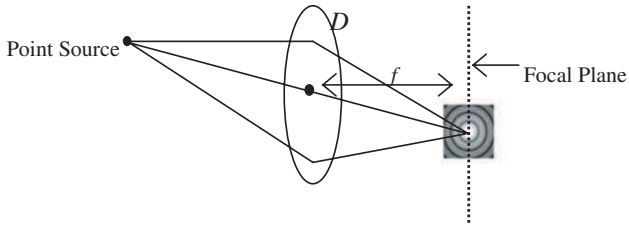

Figure 3. Image of point object.

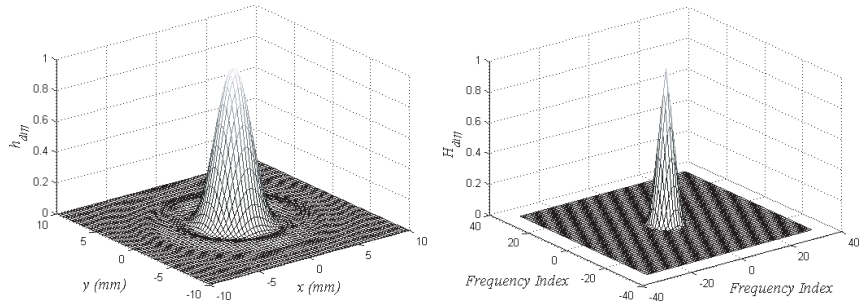

(a) (b)

Figure 4. Modeled diffraction (a) PSF and (b) MTF of the lens used in developed W-band PMMW imaging system, for specification $D = 500\,\text{mm}$, $f = 500\,\text{mm}$, $\lambda = 3.2\,\text{mm}$ (@94 GHz).

The frequency ξ, η is related to sampling frequency as follows:

$$\xi = \left(\frac{k_x}{N_x}\right) F_{sx}, \quad \eta = \left(\frac{k_y}{N_y}\right) F_{sy}, \tag{9}$$

where k_x, k_y are the spatial frequency indices and takes integer value in the interval $[\lceil -N_x/2 \rceil, \lceil N_x/2 \rceil]$ and $[\lceil -N_y/2 \rceil, \lceil N_y/2 \rceil]$ respectively. Where $\lceil x \rceil$ denote the integer value less than or equal to x. F_{sx}, F_{sy} are the sampling frequencies and N_x, N_y are the total number of sample along x- and y-axis, respectively. For fixed F_{sx}, $F_{sy} N_x$, N_y, the frequencies ξ, η are proportional to the spatial frequency indices k_x, k_y. For better presentation we used spatial frequency index instead of actual frequency.

The developed W-band PMMW imaging system, which is used here as case study [22], operates at frequency 94 GHz ($\lambda = 3.2\,\text{mm}$) and it uses a dielectric lens of diameter $D = 500\,\text{mm}$ and focal length $f = 500\,\text{mm}$. The simulated diffraction PSF and MTF of this lens are given in Figure 4. The detailed design and analysis of this lens is published in [16].

3.1.2. Lens Geometric Aberration PSF and MTF

Mathematical models [17] as well as many commercial software like V-CODE [23] is available for the calculation of aberration effect at different locations in the image plane. In this paper, we use the following Gaussian function for the aberration modeling of the lens used in W-band PMMW imaging system:

$$h_{geom}(x, y) = \frac{1}{r_{geom}^2} \exp\left(-\pi \frac{r^2}{r_{geom}^2}\right), \tag{10}$$

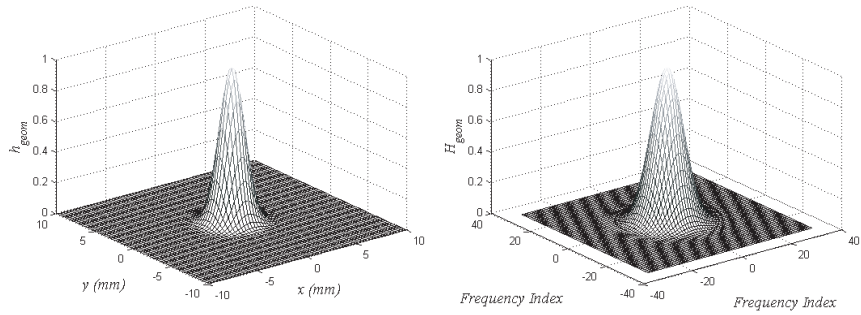

(a) (b)

Figure 5. Modeled geometric aberration (a) PSF and (b) MTF for the lens speciation given in Section 3.1.1. The geometrical scaling blur factor $r_{geom} = 4.5$.

where r_{geom} is the geometric blur scaling factor and r is same as in Eq. (7). The MTF corresponding to aberration is given as follows:

$$H_{geom}(\xi, \eta) = \exp\left(-\pi r_{geom}^2 w^2\right), \tag{11}$$

where meaning of w is same as in Eq. (8). By using CODE-V [23] software we found $r_{geom} = 4.5$ for lens specification given in Section 3.1.1. The geometric aberration PSF and corresponding MTF is shown in the Figure 5.

3.2. PSF and MTF for Linear Array of DRW Antenna

The achievable spatial resolution of a focal plane array system is an immediate consequence of the spacing of its feed elements in the focal plane of a lens. Therefore a feed with very low cross section is required. On the other hand the feed antenna must provide an efficient illumination of the lens with spillover losses as low as possible. However, this requires a highly directive antenna which would usually have a larger cross section. So it is quite challenging to design the suitable array elements that can meet these competing requirements.

We manufactured tapered DRW antenna, as in Figure 1(a), with high gain and small size, and used it as the array element in developed PMMW imaging system. The basic configuration of this antenna is characterized by a feed taper, a straight section, and a terminal taper. The feed taper establishes surface wave along the straight section, whereas the terminal taper reduces reflection caused by an abrupt discontinuity. The rectangular dielectric rod is made of high density

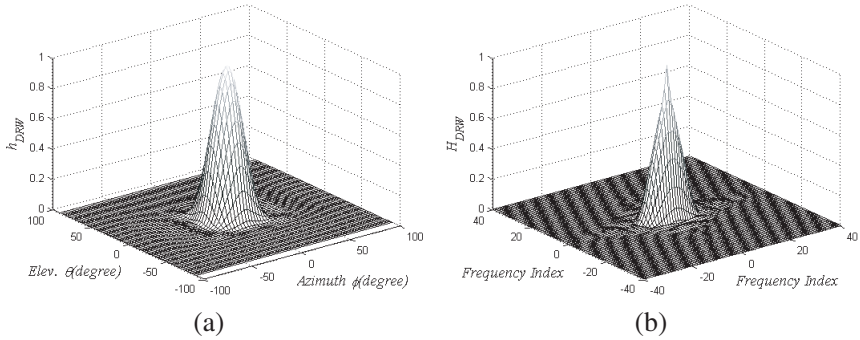

(a) (b)

Figure 6. Modeled DRW antenna (a) radiation pattern normalized, i.e., antenna PSF using CST (b) antenna MTF.

polyethylene (HDPE) and feeding is achieved by means of WR-10 metallic waveguide transition. The developed DRW antenna has gain about 15.3 dB and 10 dB bandwidth of 53.2° and 48.6° in E- and H-plane, respectively. The detail about the developed DRW antenna is published in [15].

3.2.1. Spatial Response of DRW Antenna in Linear Array

The radiation falling on the array element aperture, DRW antenna aperture, is spatially integrated. The DRW antenna aperture response is not uniform over the aperture. The incident radiation is weighted by the antenna radiation pattern before integration. Therefore, the radiation pattern of the DRW antenna is the PSF $h_{\mathrm{DRW}}(x, y)$ and its Fourier transform is the MTF. The PSF and MTF of the DRW antenna in linear array are shown in Figure 6.

3.2.2. Electromagnetic Crosstalk PSF and MTF

The other component of the array element for the linear array of DRW antenna is the electromagnetic crosstalk, which is found by calculating the mutual impedance [20, 21]. The crosstalk arises when the radiation intended for a particular array element in array contributes or induces a spurious signal on its neighbor. Crosstalk mechanism is illustrated in Figure 7. Conceptually, DRW antenna in linear array distance x apart and only the first DRW antenna receive electromagnetic radiation #0. Part of this incident radiation will be re-scattered into space #2, the other will directed towards neighboring DRW antenna as #3, where it will add vertically with incident radiation on neighboring array

element, and a part will travel into its feed as #1. Without directly receiving the incoming radiation, the neighboring array elements are excited by scattered radiation #3 by the first array element. The strength of the induced signal in neighboring array element is related to the mutual impedance [20, 21]. Because the scattered electric field of the first array element falls off with the distance, the mutual impedance tends to decrease with increasing separation. The detail mathematical analysis of mutual crosstalk for antenna array is available in classical paper [20]. The mutual impedance, Z_{12}, is calculated using equation (73) in [20], that is based on the plane wave spectrum of the far-field power radiation pattern of the antenna. This method is convenient, because, although mutual impedance is a near field phenomenon, the method in [20] requires only the knowledge of far-field power radiation pattern.

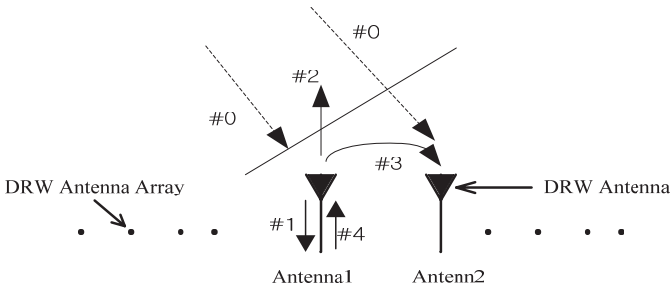

Figure 7. Schematic for the crosstalk between array elements in the linear array of DRW antenna.

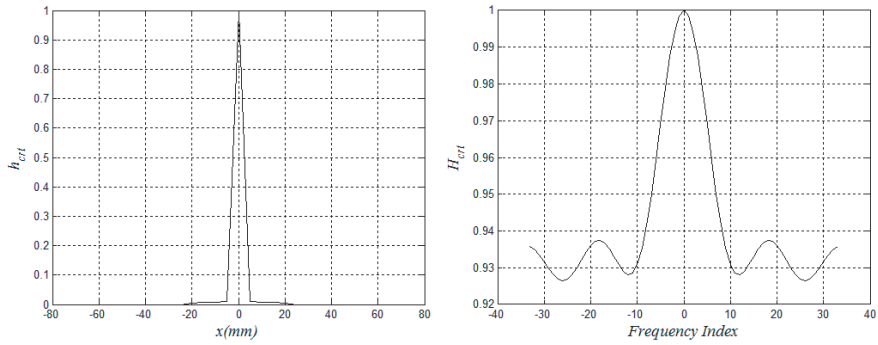

(a) (b)

Figure 8. Modeled array crosstalk. (a) PSF. (b) MTF with antenna spacing 5 mm.

We use the CST software to find out the mutual impedance for the developed linear array with DRW antenna. And we found that the inter-element back-to-back crosstalk is -39 dB for array element spacing 5 cm at 94 GHz ($\approx 1.5\lambda$). The crosstalk PSF and MTF are as in Figure 8.

3.3. PSF and MTF of Sampling Subsystem

The focal plane of the developed imaging system is sampled using linear DRW antenna and scanning. The sampling interval depends on antenna spacing in DRW antenna array and scanning. For 2-dimensional rectangular sampling grid, the sampling PSF is rectangle function whose width is equal to the sampling interval in each direction:

$$h_{sh}(x, y) = \text{rect}\left(x/x_{samp},\ y/y_{samp}\right), \tag{12}$$

where x_{samp}, y_{samp} are sampling interval in x (scan direction) and y direction, respectively. The sampling MTF:

$$H_{sh}\left(\xi, \eta\right) = \left|\text{sinc}\left(\xi x_{samp}, \eta y_{samp}\right)\right| = \frac{\sin\left(\pi\xi x_{samp}\right)}{\pi\xi x_{samp}} \frac{\sin\left(\pi\xi y_{samp}\right)}{\pi\xi y_{samp}}. \tag{13}$$

In the developed W-band PMMW imaging system, sampling interval in y-direction is fixed and equal to distance between array element, while in x-direction it depends on integration time, scanning speed, and scene motion. Here, we assume that scene is not in motion, i.e., image of scene in focal plane is static. In this case, the sampling interval in x-direction is:

$$x_{samp} = v_{scan}\tau, \tag{14}$$

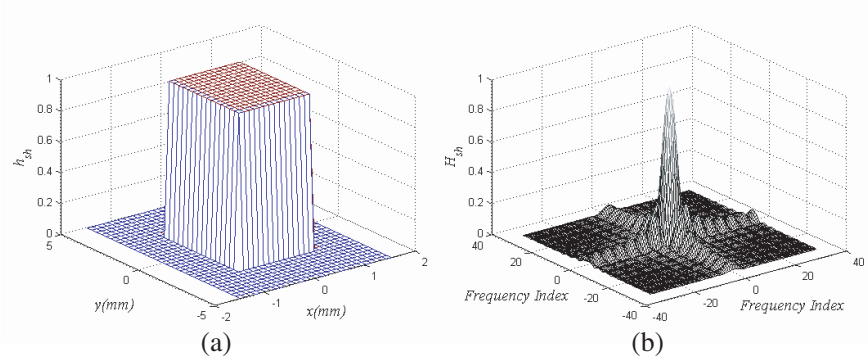

(a) (b)

Figure 9. Modeled sampling. (a) PSF and (b) MTF for spacing between antenna in array is 5 mm, i.e., $y_{samp} = 5$ mm, $v_{scan} = 150$ mm/s, and $\tau = 10$ ms.

where v_{scan} is the scan velocity, τ is the integration time. In the developed system spacing between antenna in array is 5 mm, i.e, $y_{samp} = 5\,\text{mm}$, $v_{scan} = 150\,\text{mm/s}$, and $\tau = 10\,\text{ms}$. Thus, $x_{samp} = 1.5\,\text{mm}$. The sampling PSF and MTF are shown in Figure 9.

4. MEASUREMENT AND OPTICAL PERFORMANCE ANALYSIS

Figure 10 shows the schematic and experimental setup for the measurement of the lens PSF and over all PSF for the quasi optical part used in the developed W-band PMMW imaging system. This experiment setup was established for the near field measurement. We used W-band source generator with source locking counter and

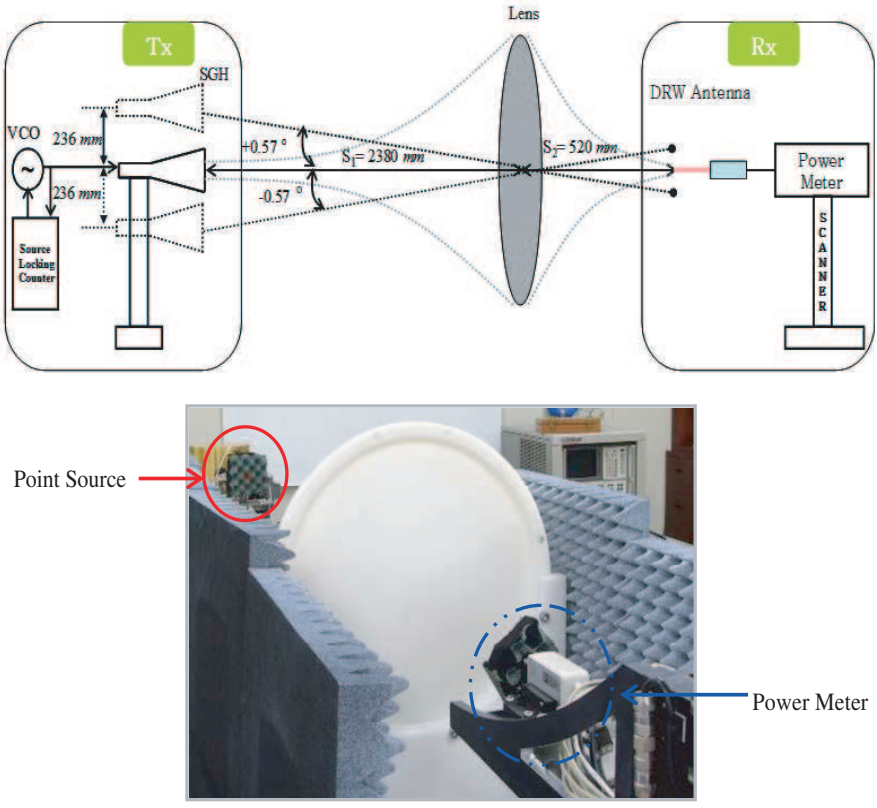

Figure 10. Schematic and photo of experimental setup for PSF and resolution measurement.

a pyramidal standard gain horn (SGH) (Millitech Co, aperture size $24 \times 18\,\text{mm}^2$) as point source transmitter. SGH is mounted on a scanning stand, which is equipped with measurement scale in order to get position of SGH from reference point (optical axis of lens). The combination of lens and DRW antenna array used as a receiver. The W-band power meter is attached to the end of DRW antenna in antenna array to measure the received power.

This initial experiment setup is for fixing focal plane and image plane. The SGH is fixed at a distance $S_1 = 2380\,\text{mm}$ from lens and at height same as optical axis of the lens. DRW antenna scanned along optical axis of the lens until the maximum output power of the feed was observed by the W-band power meter. The maximum received power was obtained at feed position $S_2 = 520\,\text{mm}$ (Figure 10), and it is considered as beam focal point/image point of the lens corresponding to the source point. The focal length, f, was calculated using lens formulae, $\frac{1}{S_1} + \frac{1}{S_2} = \frac{1}{f}$, and found $\approx 427\,\text{mm}$. The difference between the measured focal length (427 mm) and design focal length (500 mm) can be due to combined effect of following factors: i) Error in the measurement of the dielectric constant of HDPE at W-band. ii) Due to large size of lens, surface curvature is not correctly manufactured. iii) Spherical aberration. iv) Measurement error.

Next, the feed antenna (DRW) array is positioned at the focus point of the lens in order to measure the PSF, crosstalk effect, Rayleigh resolution limit, and diffraction limited nature of the imaging subsystem.

The PSF measured by translating the single feed antenna and antenna array in the focal plane for following two cases: i) using single feed antenna: Lens and feed antenna effect, and ii) using antenna array: Lens, feed antenna, and crosstalk effect. Figures 11(a), 11(b) shows the cross section of simulated and measured PSF at dB and linear scale. From simulation we found that the sampled-imaging subsystem is almost symmetric, hence we presented a cross section PSF for analysis.

The modeled and measured PSF, $h(x, y)$, for case i and ii are shown in Figure 11. The modeled and measured PSF closely agreed for both cases. It is evident from Figure 11 that the measurement for case i and ii differed nominally, thus crosstalk effect is almost negligible, and hence, it is not serious problem for the developed DRW antenna array. The modulation transfer function (MTF) shown in the Figure 12 corresponding to the PSF in Figure 11. The close agreement between measurement and theoretical diffraction-limited PSF and MTF curves indicates that the optics is diffraction-limited and the pattern is adequately sampled.

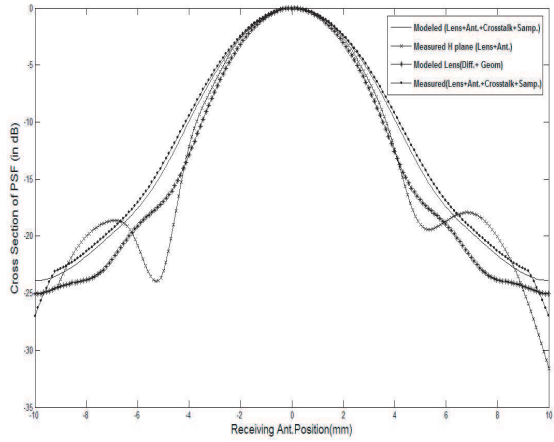

(a)

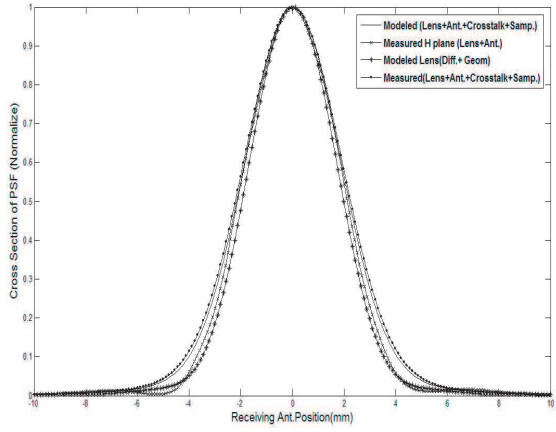

(b)

Figure 11. Measured PSF by translating single DRW antenna and array of antenna. (a) dB scale and (b) linear scale.

According to the *Rayleigh criterion* of resolution, two incoherent point sources in object plane are "barely resolved" by diffraction limited system with a circular aperture in image plane, when the center of the PSF and diffraction pattern generated by one point source falls exactly on the 1st zero of the PSF pattern generated by the 2nd source. Figure 10 shows the schematic of measurement for resolution of the imaging subsystem. The measurement data is shown in Figure 13. From measured data, it is clear that *Rayleigh criterion* hold for object angular separation 0.57° (≈ 2.36 mm) in object space at distance 2380 mm.

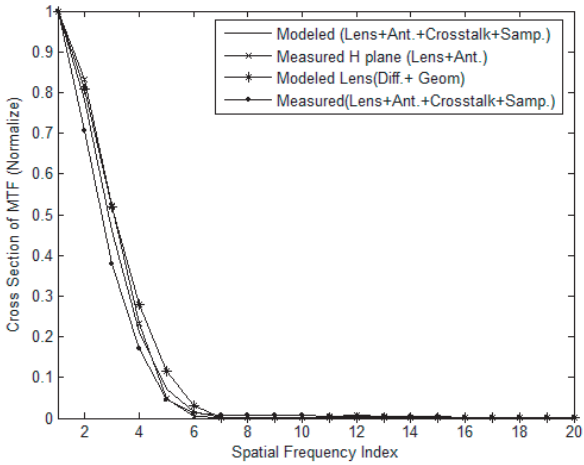

Figure 12. The MTF corresponding to the measured and simulated PSF.

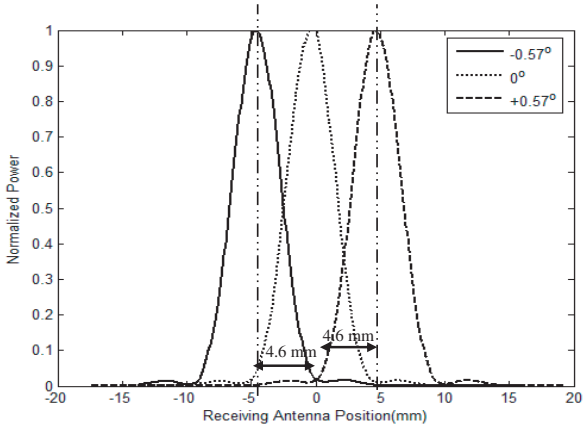

Figure 13. Measured power for object angular separation $-0.57°$, $0°$, and $+0.57°$ as in Figure 10.

Theoretically, the minimum resolvable separation in the image plane is given as follows [17, 18]:

$$\delta = \frac{1.22\lambda f}{D}, \tag{15}$$

where D is aperture diameter, λ is wavelength, and f is the focal length. Theoretical value of $\delta = 3.904\,\text{mm}$ for developed quasi optics system, while measured value is of resolvable separation in is 4.6 mm.

This error in theoretical and measurement may be measurement error or due to effect of feed horn used during measurement.

5. CONCLUSION

This paper presents performance analysis of imaging system based on linear array of focused receiver. This approach accounts for the combined effect of dielectric lens, dielectric rod waveguide (DRW) antenna in array, crosstalk between DRW antenna in array, and sampling. We modeled these effects using concept of point spread function (PSF) and modulation transfer function (MTF). And the performance analysis of PMMW imaging system at W-band using PSF and MTF is presented.

As a case study, we used quasi optics based W-band PMMW imaging system that exploits a new type of DRW antenna, which has higher gain, in linear array of focused receiver. Antenna-to-antenna crosstalk causes a modest MTF decrease at low spatial frequencies, where as the narrow PSF causes modest MTF gain at high frequencies. From simulation and measurement, we found that overall electromagnetic crosstalk will not be a significant image quality/imaging performance factor in the used linear array of DRW antenna. Thus, the developed linear array with DRW antenna is suitable for passive imaging application at W-band.

An experimental setup for measuring PSF is presented. The close agreement between measured and theoretical PSF and MTF curves indicates that the system is diffraction-limited and the pattern is adequately sampled. We measured minimum resolvable separation in image plane 4.6 mm, which is also close to the sampling by antenna array ($5\,\text{mm} \approx 1.5\lambda = 4.80\,\text{mm}$). This also confirms the adequate sampling of the pattern. Thus, the proposed imaging system is efficient and it has almost diffraction limited resolution.

In this paper, we assumed that system is linear and shift-invariant (isoplanatic), i.e., the PSF (hence MTF) does not depend on the location and the strength of a point source. If the shift-invariant assumption is not valid, the image/response of point source, PSF, will depend on its location, and the system MTF will have spurious location-dependent phase dependence. The test for shift-variant nature and PSF/MTF approach to system performance analysis for the developed system is our future plan.

This paper is based on development of Millimeter wave Imaging Radiometer Equipment (MIRAE) [22] by Sensor System Laboratory at GIST Republic of Korea.

ACKNOWLEDGMENT

This work was supported by the Dual Use Center and Millisys Inc. (http://www.millisys.com) through the contract GM03980 at the Gwangju Institute of Science and Technology and the BK-21 program of government of Republic of Korea. Thank to Dr. Tanveer J. Siddiqui, for many useful discussion in order to improve the overall paper quality.

REFERENCES

1. Yujiri, L., M. Schoucri, and P. Moffa, "Passive millimeter-wave imaging," *IEEE Microwave Magazine*, Sep. 2003.
2. Wilson, W. J., R. J. Howard, and A. C. Ibbot, "Millimeter-wave imaging sensor," *IEEE Trans. on Microwave Theory and Techniques*, Vol. 34, No. 10, 1026–1035, 1986.
3. Lovberg, J., R. Chou, and C. Martin, "Real-time millimeter-wave imaging radiometer for avionics synthetic vision," *Proc. SPIE Conf. on Sensing, Imaging, and Vision for Control and Guidance of Aerospace Vehicles*, J. G. Verly and S. S. Welch (eds.), Vol. 2220, 234–244, 1994.
4. Richter, J., D. Notel, F. Kloppel, J. Huck, H. Essen, and L.-P. Schmidt, "A multi-channel radiometer with focal plane array antenna for W-band passive millimeter wave imaging," *IEEE MTT-S Int. Microwave Symp. Dig.*, 2006.
5. Appleby, R., R. N. Anderton, S. Price, N. A. Salmon, G. N. Sinclair, J. R. Borrill, P. R. Coward, P. Papakosta, A. H. Lettington, and D. A. Robertson, "Compact real-time (video rate) passive millimeter-wave imager," *Proc. SPIE Conf. on Passive Millimeter-wave Imaging Technology III*, Vol. 3703, 13–19, 1999.
6. Yujiri, L., H. Agravante, M. Biedenbender, G. S. Dow, M. Flannery, S. Fornaca, B. Hauss, R. Johnson, R. Kuroda, K. Jordan, P. Lee, D. Lo, B. Quon, A. Rowe, T. Samec, M. Shoucri, K. Yokoyama, and J. Yun, "Passive millimeter-wave camera," *Proc. SPIE Conf. on Passive Millimeter-wave Imaging Technology*, Vol. 3064, 15–22, Orlando, 1997.
7. Yujiri, L., H. Agravante, S. Fornaca, B. Hauss, R. Johnson, R. Kuroda, B. Quon, A. Rowe, T. Samec, M. Shoucri, and K. Yokoyama, "Passive millimeter wave video camera," *Proc. SPIE Conf. on Passive Millimeter-wave Imaging Technology II*, Vol. 3378, 15–22, 1998.

8. Rutledge, D. B. and M. S. Muha, "Imaging antenna arrays," *IEEE Trans. on Antennas and Propagation*, Vol. 30, No. 4, 1982.
9. Goldsmith, P. F., C. T. Hsieh, and G. R. Huguenin, "Focal plane imaging systems for millimeter wavelengths," *IEEE Trans. on Microwave Theory and Techniques*, Vol. 41, No. 10, 1664–1675, 1993.
10. Qassim, K. A. S., "Optimization of focal plane arrays for microwave imaging; printed yagi, dielectric rod and constant width slot antennas are investigated and optimized for close stacking in focal plane arrays intended for microwave imaging," Ph.D. Dissertation, University of Branford, UK, Bradford, 1992.
11. Dow, G. S., T. N. Ton, H. Wang, D. C. W. Lo, W. Lam, B. Allen, K. L. Tan, and J. Berenz, "W-band MMIC direct detection receiver for passive imaging," *IEEE MTT-S Int. Microwave Symp. Dig.*, 163, 1993.
12. Kuroda, R. T., G. S. Dow, D. Moriarty, R. Johnson, A. Quil, S. D. Tran, V. Pajo, S. Fornaca, and L. Yujiri, "Large scale W-band focal plane array developments for passive millimeter wave imaging," *Proc. SPIE Conf. on Passive Millimeter-wave Imaging Technology II*, Vol. 3378, 75–62, Orlando, FL, 1998.
13. Richter, J. and L.-P. Schmidt, "Dielectric rod antennas as optimized feed elements for focal plane array," *Proceeding of the IEEE AP-S International Antennas and Propagation Symposium*, Vol. 3A/4, Washington, D.C., USA, Jul. 2005.
14. Lioubtchenko, D. V., S. N. Dudorov, J. Mallat, and A. V. Raisanen, "Dielectric rod waveguide antenna for W band with good input match," *IEEE Microwave and Wireless Components Letters*, Vol. 15, No. 1, 2005.
15. Kim, W. G., J. P. Thakur, and Y.-H. Kim, "Efficient DRW antenna for quasi-optics feed in W-band imaging radiometer system," *Microwave and Optical Technology Letters*, Vol. 52, No. 5, 1221–1223, 2010.
16. Thakur, J. P., W.-G. Kim, and Y.-H. Kim, "High resolution large aperture aspheric dielectric lens antenna for W-band quasi-optics," *Progress In Electromagnetics Research*, PIER 103, 57–65, 2010.
17. Vollmerhausen, R. H. and R. G. Driggers, *Analysis of Sampled Imaging Systems*, Vol. TT39, ISBN 0-8194-3489-2, SPIE Press, 2000.
18. Boreman, G. D., *Modulation Transfer Function in Optical and Elctro-optical Systems*, Vol. TT52, ISBN 0-8194-4143-0, SPIE Press, 2001.

19. Goodman, J. W., *Introduction to Fourier Optics*, McGraw-Hill, 1997.
20. Wasylkiwskyj, W. and W. K. Kahn, "Theory of mutual coupling among minimum-scattering antennas," *IEEE Trans. on Antennas and Propagation*, Vol. 18, No. 2, 1970.
21. Balanis, C. A., *Antenna Theory Analysis and Design*, 3rd edition, Wiley & Sons, 2005.
22. Kim, W.-G., N.-W. Moon, Y.-J. Kim, J.-M. Jung, M.-K. Jung, Y.-S. Chang, M.-S. Park, and Y.-H. Kim, "Development of 30 channels millimeter wave imaging radiometer equipment (MIRAE)," *Proceeding of International Symposium on Remote Sensing*, Busan, South Korea, Oct. 2009.
23. http://www.opticalres.com/.